

Green synthesis of zinc oxide nanoparticles using Aloe Vera plant for investigation of antibacterial properties

Received 5th November 2019,
Accepted 4th January 2020,
DOI:10.22126/anc.2020.4745.1016

Hadi Mofid ^{*,1}, Mirabdollah Seyed Sadjadi ¹, Moayed Hossaini Sadr ², Alireza Banaei ³,
Nazanin Farhadyar ⁴

¹ Department of Chemistry, Science and Research Branch, Islamic Azad University, Tehran, Iran.

² Department of Chemistry, Azarbaijan Shahid Madani University, Tabriz, Iran.

³ Department of Chemistry, Payame Noor University, Tehran, Iran.

⁴ Department of Chemistry, Varamin Pishva Branch, Islamic Azad University, Varamin, Iran.

Abstract

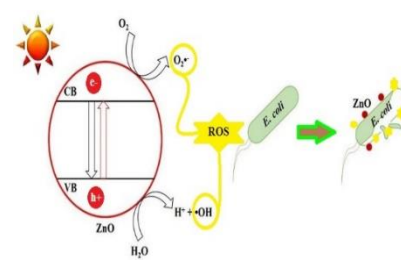
In this paper, we report the green synthesis of ZnO nanoparticles by using the medicinal plant, *Aloe Vera*. Characterization of the prepared nanoparticles was carried out by various techniques such as field emission scanning electron microscopy (FESEM), elemental analysis (EDS), X-ray diffraction (XRD), ultraviolet-visible (UV-Vis), and Fourier-transform infrared (FTIR). The synthesized nanoparticles have the hexagonal wurtzite structure of an average grain size of 17 nm confirmed from X-ray diffraction analysis. Studies of antibacterial activity show that the synthesized ZnO nanoparticles have potential applications in this field. For antibacterial studies, we used *Bacillus Subtilis* and *Staphylococcus Aureus* as the gram-positive and *Escherichia Coli* and *Salmonella Typhi* as the gram-negative bacteria.

Keywords: Green synthesis, *Aloe Vera*, Antibacterial properties.

Introduction

The field of nanotechnology is one of the most active researches in modern material science. Nowadays, nanoscience, as well as nanotechnology, is widely applied in different fields mainly in sensor, electronic, antibacterial, water purification, cosmetic, biomedical, pharmaceutical, environmental, catalytic and material applications.¹⁻⁹ The zinc oxide (ZnO) has high electron mobility, high thermal conductivity, good transparency, wide and direct bandgap (3.37 eV), and large exciton binding energy; it can also be grown easily in various nanostructure forms.¹⁰ The size, crystallinity, and morphology of the nonmaterial can greatly influence their catalytic, magnetic, electronic, and optical properties.¹¹ The ZnO nanoparticles (NPs) are of significant interest as they provide many practical applications worldwide.¹² Recently green synthesis has become a popular way to synthesize these NPs due to its low cost, environment compatibility, synthesizable in ambient atmosphere and non-toxicity.¹³ The antibacterial activity of ZnO NPs has been ascribed to a variety of factors like abrasiveness of the nanomaterial's, presence of surface defects, orientation and facet formation, possible disruption of the cell membrane, oxidative stress created inside the cell, generation of reactive oxygen species (ROS), lattice constant of the particles, etc.¹⁴⁻¹⁸

Biological methods of synthesis of nanomaterial's are considered to be environmentally safe and sound compared to the conventional synthetic methods.^{19,20} Since plants are rich in polyphenols, they serve as important materials for the production of metallic NPs.²¹ Such types of synthesis using phytochemicals minimizes or



eliminates chemical interventions, thereby resulting in a truly green and non-polluting eco-friendly process.^{22,23} Here we report the new fast method to green synthesis of ZnO NPs and their antibacterial properties against both gram-negative and gram-positive bacteria.

Experimental

Antibacterial activity

The disc diffusion method was applied to examine antibacterial activity.²⁴ Ciprofloxacin and fluconazole were taken as a standard for antibacterial activity. A panel of 4 common pathogenic microorganisms with two gram-positive bacteria *Staphylococcus Aureus* (PTCC 1431), *Bacillus Subtilis* (PTCC 1156) and two gram-negative bacteria *Escherichia Coli* (PTCC 1553), *Salmonella Typhi* (PTCC 1609) was used. The bacterial strains were obtained from the Persian Type Culture Collection, IROST, Iran.

Preparation of the Aloe Vera leaf extract (ALE)

Aloe Vera leaf (40 g) were thoroughly washed, dried and then boiled in 80 ml of deionized water for half an hour. The color of the aqueous solution changed from watery to dark yellow. The extract was cooled at room temperature, filtered through Whatman filter paper and stored at 20 °C for further use.

Synthesis of ALE-capped ZnO NPs

For the synthesis of ZnO NPs, 0.4 g of Zn(OAC)₂ were dissolved in 50 mL deionized (DI) water. Then 4 mL of ALE were added and the resulting mixture stirred for 20 min using a magnetic stirrer. In order to adjust the pH of the solution to pH 12, NaOH solution 2 M was added drop-wise while stirring. After the end of the reaction,

Corresponding author:

Hadi Mofid, Email: hadimofid@yahoo.com

Table 1. Anti-bacterial activity of the ZnO NPs vs. Aloe Vera extract.

Bacteria	Category	Zone of Inhibition (mm)					
		Sample A (Aloe Vera)			Sample B (ZnO)		
		5 mg	10 mg	25 mg	5 mg	10 mg	25 mg
Escherichia Coli	Gram negative	2	3	5	11	13	16
Salmonella Typhi	Gram negative	1	2	4	9	14	17
Bacillus Subtilis	Gram Positive	5	8	13	13	17	23
Staphylococcus Aureus	Gram Positive	8	12	17	15	21	25

the white crystalline precipitated were collected by filtration and washed several times with hot water and dried at room temperature. Then placed in a furnace at 600°C for 1 hour after annealed in an oven at 120 °C for 3-5 h.

UV-Vis Spectroscopy

The ultraviolet-visible (UV-Vis) spectrum of the synthesized ZnO NPs was carried out on a Shimadzu 1601-PC UV/Vis spectrophotometer.

X-ray diffraction measurements

The X-ray diffraction (XRD) pattern of powdered ZnO NPs was recorded on Philips X'Pert PRO XRD system (Netherlands) at 40 kV with CuK α radiation ($k = 1.54 \text{ \AA}$). X'pert high score database used to check for the references. The crystalline size of the ALE-ZnO NPs was calculated following the Debye–Scherer’s formula (equation (1)).

Scanning electron microscopy (SEM)

SEM analysis was carried out using the fine powder of ZnO NPs by use of Phenom ProX ultimate all-in-one imaging and X-ray energy dispersive spectroscopy (EDS) system (Netherlands) at an accelerating voltage of 15 kV.

Fourier-transform infrared (FTIR) spectroscopy

FTIR was employed for the assessment of functional groups on ZnO NPs. Briefly, the air-dried powder of ZnO NPs were mixed with spectroscopic grade KBr (1:100) and their spectrum was recorded. FTIR measurements were carried out by the use of the Shimadzu prestige-21 FTIR spectrophotometer (4000–400 cm^{-1}).

Results and discussion

X-ray diffraction analysis

Figure 1 shows distinctive Bragg reflections at 2θ values of 31.887, 34.576, 36.400, 47.657, 56.723, 63.032, 66.500, 68.096, 69.312, 72.712, and 77.052 can be indexed to the (100), (002), (101), (102), (110), (103), (200), (112), and (201) that are in good agreement with wurtzite ZnO.²³ The distinct and clear peaks confirmed the high purity and crystalline nature of the prepared ZnO NPs. The

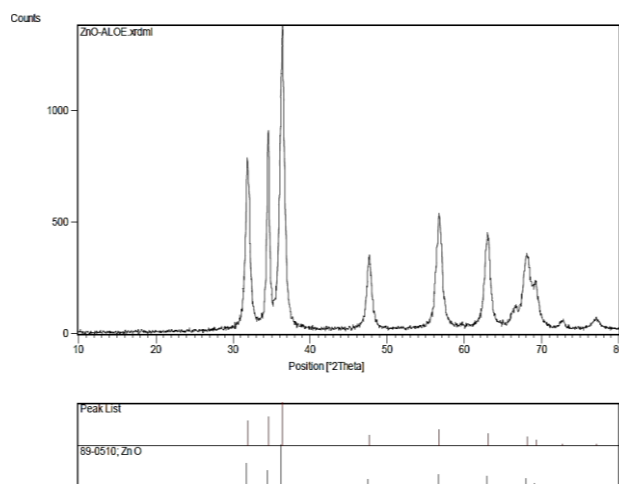


Figure 1. The XRD pattern of the synthesized ZnO NPs.

crystalline size has been estimated from the broadening of the first diffraction peak using the Debye–Scherer formula:²⁵

$$D = 0.9\lambda / \beta \cos\theta \quad (1)$$

where D is the crystal size of ZnO NPs, 0.9 is Scherer’s constant, λ is the wavelength of X-rays (1.541 \AA), θ is the Bragg diffraction angle, and β is the full-width at half-maximum (FWHM) of the diffraction peak corresponding to plane (101). The average particle size of the sample was found to be 16.98 nm which is derived from the FWHM of the more intense peak corresponding to the (101) plane located at 36.4006° using Scherer’s formula.

$$\beta = 0.49204 * 22 / 180 * 7 = 0.00859 \text{ radians} \quad (2)$$

$$2\theta = 36.4006 \rightarrow \theta = 18.2003$$

$$D = 0.9\lambda / \beta \cos\theta \rightarrow D = 0.9 * 0.154 / 0.00859 \cos(18.2003) = 16.98 \text{ nm}$$

Scanning electron microscopy

The SEM images exhibited pleomorphic ZnO NPs (Figure 2). The elemental composition of ZnO NPs was analyzed through EDX and

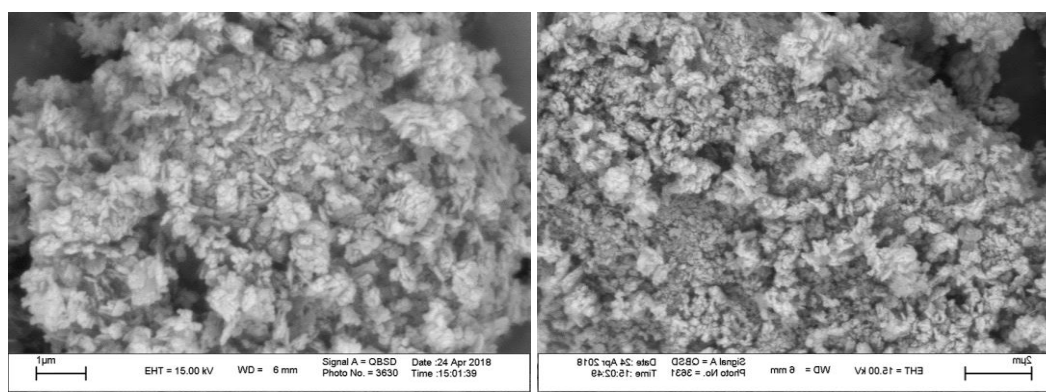


Figure 2. The SEM image of synthesized ZnO NPs.

found comprised of zinc (48.6%) and oxygen (51.4%) by atomic concentration (Figure 3). Results indicate three emission peaks of metallic zinc and small peaks of oxygen, which confirmed the formation of ZnO NPs.

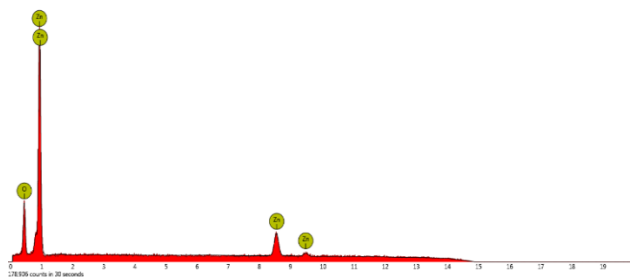


Figure 3. The EDS pattern of synthesized ZnO NPs.

FTIR spectroscopy

The FTIR spectrum of ZnO NPs is shown in (Figure 4). This spectrum exhibited a broad peak at 3437 cm^{-1} , assigned to the -OH group from phenol present in the extract. The bands at 3452 and 2929 cm^{-1} are attributed to stretching vibrations of the amines, O-H stretching of alcohols, and C-H stretching of alkanes. A similar band pattern has been reported by Sangeetha et al.²⁴ for the ZnO NPs synthesized by *A. barbadensis miller* leaf extract. The peak at 1608 cm^{-1} is due to the amide regions that are characteristics of proteins and enzymes. The high-intensity band around 440 cm^{-1} is due to stretching of zinc and oxygen bond.²⁶

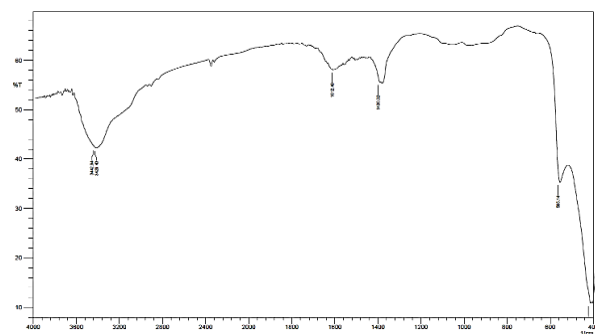


Figure 4. The FTIR spectra of synthesized ZnO NPs.

UV-Vis spectroscopy

The UV-Vis spectrum is shown in Figure 5. Confirmation of the synthesized ZnO nanoparticles was exhibited by the blue-shifted absorption maximum at 372 nm . Bulk ZnO exhibits absorption maximum around 380 nm approximately.²⁷

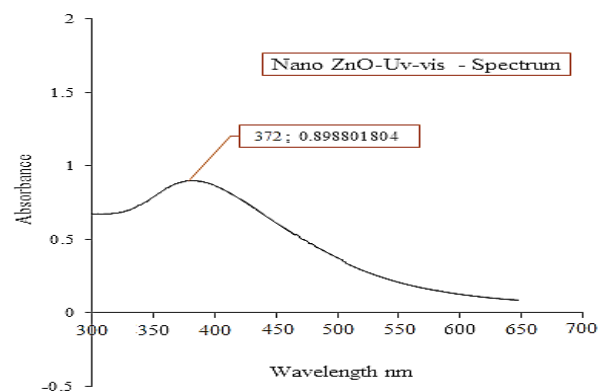


Figure 5. The UV-Vis spectrum of synthesized ZnO NPs.

Antibacterial test

The antibacterial activity of the synthesized ZnO NPs was tested for gram-positive and gram-negative bacteria. The results are shown in Table 1 that represent the excellent antibacterial activity of ZnO NPs against all gram-positive and gram-negative bacteria. The experimental outcomes undeniably suggest an effective growth inhibitory activity of the ZnO NPs upon the micro-organisms.

Conclusion

Effective green synthesis of nanoparticles will have greater implication and applications in biomedical research. In this study, ZnO NPs were synthesized by using *Aloe Vera* leaf extract. The phytochemicals present in the plants reduced zinc acetate. The crystalline structure of ZnO NPs was confirmed by XRD. The Antibacterial studies confirmed that the synthesized ZnO NPs have effective growth inhibitory activity upon the micro-organisms.

Aknowldgement

The authors express their thanks to the research vice presidency of Science and Research Branch, Islamic Azad University for encouragement, and financial supports.

References

1. V. Vadlapudi and Kaladhar D.S.V.G.K, *Middle-East J. Sci. Res.* **19**, **2014**, 834.
2. S.H. Lee, W.-Y. Rho, S.J. Park, J. Kim, O.S. Kwon, and B.-H. Jun, *Sci. Rep.* **8**, **2018**, 16763.
3. A.M. Allahverdiyev, E.S. Abamor, M. Bagirova, and M. Rafailovich, *Future Microbiol.*, **6**, **2011**, 933.
4. K. Adibkia, M. Barzegar- Jalali, A. Nokhodchi, M. Siah Shadbad, Y. Omid, Y. Javadzadeh, and G. Mohammadi, *J. Pharm. Sci.*, **15**, **2010**, 303.
5. R.K. Bera, S.M. Mandal, and C.R. Retna, *Lett. Appl. Microbiol.*, **58**, **2014**, 520.
6. B. Kakavandi, A. Jonidi, R. Rezaei, S. Nasser, A. Ameri, and A. Esrafiy, *Iran. J. Environ. Health Sci. Eng.*, **10**, **2013**, 19.
7. A. Desireddy, B.E. Conn, J. Guo, B. Yoon, R.N. Barnett, B.M. Monahan, K. Kirschbaum, W.P. Griffith, R.L. Whetten, U. Landman, and T.P. Bigioni, *Nature*, **501**, **2013**, 399.
8. L. Wang, T. Zhang, P. Li, W. Huang, J. Tang, P. Wang, J. Liu, Q. Yuan, R. Bai, B. Li, and K. Zhang, *ACS Nano*, **9**, **2015**, 6532.
9. F.J. Heiligtag and M. Niederberger, *Research. Mater. Today*, **16**, **2013**, 262.
10. M. Kashif, M.E. Ali, S.M. Usman Ali, U.Hashima et al., *Ceram. Int.*, **2013**, **39**, 6461.
11. S. Tachikawa, A. Noguchi, T. Tsuge, M. Hara, O. Odawara, and H. Wada, *Materials*, **4**, **2011**, 1132.
12. A. Awwd, N. Salem, and M. Abdeen, *Int. J. Indust. Chem.*, **4**, **2013**, 29.
13. Y. Zhang, D. Yang, Y. Kong, X. Wang, O. Pandoli, and G. Gao, *Nano. Biomed. Eng.*, **2**, **2010**, 252.
14. Y. Xie, Y. He, P.L. Irwin, T. Jin, and X. Shi, *Appl. Environ. Microbiol.* **77**, **2011**, 2325.
15. O. Yamamoto, M. Komatsu, J. Sawai, and Z-E.Nakagawa, *Mater Sci.* **15**, **2004**, 847.
16. R.K. Dutta, B.P. Nenavathu, M.K. Gangishetty, and A.V.R. Reddy, *Colloids Surf. B*, **94**, **2012**, 143.
17. Y. Li, W. Zhang, J. Niu, and Y. Chen, *ACS Nano*, **6**, **2012**, 5164.
18. G. Apperrot, A. Lipovsky, R. Dror, N. Perkas, Y. Nitzan, R. Lubart, and A. Gedanken, *Adv. Funct. Mater.*, **19**, **2009**, 842.

19. D. Bhattacharya and R.K. Gupta, *Crit. Rev. Biotechnol.*, **25**, **2005**, 199.
20. P. Mohanpuria, N.K. Rena, and S.K. Yadav, *J. Nanoparticle Res.*, **10**, **2008**, 507.
21. S.K. Nune, N. Chanda, R. Shukla, K. Katti, R.R. Kulkarni, S. Thilakavathi, S. Mekapothula, R. Kannan, and K.V. Katti, *J. Mater. Chem.*, **19**, **2009**, 2912.
22. G. Ghodake, C. Eom, S.W. Kim, and E. Jin, *Bull. Korean Chem. Soc.*, **31**, **2010**, 2771.
23. A.W. Bauer, W.M.M. Kirby, J.C. Sherris, and M. Turck, *Amer. J. Clin. Pathol.*, **45**, **1966**, 493.
24. A.L. Patterson, *Phys. Rev.*, **56**, **1939**, 978.
25. Y.J. Kwon, K.H. Kim, C.S. Lim, and K.B. Shim, *J. Ceram.Proc. Res.*, **3**, **2002**, 146.
26. H. McMurdie, M. Morris, E. Evans, B. Paretzkin, W. Wong-Ng, L. Ettliger, and C. Hubbard, *Powder Diffraction*, **1**, **1986**, 76.
27. G. Sangeetha, S. Rajeshwari, and R. Venckatesh, *Mater. Res. Bull.*, **46**, **2011**, 2560.